

Supplementary Material

Robustness, Flexibility, and the Role of Lateral Inhibition in the Neurogenic Network

Eli Meir, George von Dassow, Edwin Munro,
and Garrett M. Odell

Supplementary Results and Discussion

Genes Involved in the Neurogenic Network

The first step in making a model of a genetic network is to construct a “wiring diagram” of the genes and gene products involved and the connections between these representing their interactions. This paper concerns the neurogenic network and its role in selecting single neuroblasts (NB) and sensory organ precursors (SOP) from proneural clusters in *Drosophila* embryos and their imaginal disks. The next few paragraphs outline the central loop of the network used in this process, as understood currently in the literature. There follow discussions of some of the important genes outside this loop that influence the positions of the SOPs. The core genes and their interactions are all summarized in the diagram in Figure 1. Many other reviews exist of various pieces of the neurogenic network. Here, we attempt a thorough summary of current literature to justify all the connections in Figure 1 and some of the modeling choices we make in the main text. Readers unfamiliar with the neurogenic network may find it more profitable to skip this section and simply refer to Figure 1.

Two genes, *achaete* (*ac*) and *scute* (*sc*), appear to be the primary determinants of neural fate. Cells expressing high levels of *Ac* and *Sc* proteins become neural, while others adopt an epidermal fate [S1]. *Ac* and *Sc* both belong to a family of transcription factors that contain a conserved basic helix-loop-helix region (bHLH). The family members use the bHLH domains to dimerize with one another [S2, S3], becoming transcriptionally active only as dimers. *Ac* and *Sc* both bind to the bHLH cofactor Daughterless (*Da*) and, as heterodimers with *Da*, each of these can activate both its own and each other’s transcription [S4–S7].

Both *Ac* and *Sc*, as heterodimers with *Da*, directly activate transcription of the *Delta* (*Dl*) gene [S8–S10]. *Delta* protein is a transmembrane ligand that can bind to and activate its receptor protein Notch (*N*) in neighboring cells [S11]. There is some evidence that *Dl* can also bind to *N* within the membrane of the same cell, though it is not clear whether this intracellular binding can activate *N* [S11]. What seems clearer is that intracellular interactions between *Dl* and *N* can inhibit *N* activity in that cell, even in the presence of *Dl* in neighboring cells [S12, S13]; also see [S14] for evidence that another *N* ligand, *Serrate*, does the same. Recently, both [S15] and [S16] showed that *Dl* is cleaved at the membrane by the protein Kuzbanian, forming extracellular *Dl* fragments that are biologically active and exist *in vivo*. These results make it likely that, in at least some cases, a cleavage product of the *Dl* protein diffuses and may be able to act at a distance from the cells that expressed it. But, as it has yet to be shown that *Dl* diffusion plays a role in the processes explored in this paper, we omit *Dl* diffusion between cells in the model we present here. We include diffusion of both *Dl* and *N* between different faces of the same cell.

Notch (*N*) is a transmembrane receptor molecule produced in nearly constant quantities across broad fields of cells [S17]. Regulation of *N* production per se does not seem to play a role in the neurogenic patterning mechanism [S18]; although, in some patterns involving this network, the concentration of *N* is regulated [S19]. In our model, we assume constitutive expression of *N* in all cells. When *N* is activated by binding to its ligand *Dl*, it has the effect of reducing the production of *ac* and *sc*. The members of the pathway between *N* and *ac/sc* are well known, but the way they interact is still somewhat confusing. There is now fairly good evidence that, upon binding *Dl*, an intracellular portion of *N* is cleaved and transported to the nucleus

[S20]. This cleaved portion of *N* may be transcriptionally active on its own, but at least some of Notch’s activity is due to interactions with the Suppressor of Hairless (*Su(H)*) protein, a known transcription factor [S21, S22]. When activated by the cleaved fraction of *N*, *Su(H)* in turn upregulates the transcription of some genes in the *Enhancer of split complex* (*E(spl)*), a group of seven bHLH transcription factors that act as repressors of, among other genes, *ac* and *sc* transcription [S23–S26]. This repression of *ac* and *sc* by *E(spl)* completes the loop.

In the models here, we chose to ignore the growing body of work on the details of *N* activation and cleavage and model it as a simple dimerization between *N* and *Dl*, after which the dimer enters the cytoplasm and interacts with *Su(H)*. This is functionally equivalent to *N* being cleaved upon contact with *Dl*, with an intracellular portion becoming active (*Ndl* in Figure 1) and the extracellular portion of *N*, together with the *Dl* molecule it bound, degrading with no further activity.

Su(H) is normally found in the nucleus and is distributed nearly uniformly among cells in each proneural cluster [S27]. Recent work on both peripheral neurogenesis and eye development shows that *Su(H)* is normally a transcriptional repressor but becomes a transcriptional activator when bound by an activated *N* fragment in the nucleus [S28, S29]. Loss-of-function *Su(H)* mutants do not express *E(spl)* genes, though, even in the presence of activated Notch, and adding *Su(H)* alone produces a slight increase in *E(spl)* transcription [S25]. Similarly, removing the *Su(H)* repressor *Hairless*, which binds to and inactivates *Su(H)*, leads to an increase in *E(spl)* production [S30]. Thus, in our models here, we have only included the activator function of *Su(H)* in combination with *N*, and we left out the repression function. Further, for simplicity, our model assumes a never-changing amount of *SU(H)* protein, some of which is complexed with *N*. This is equivalent to, but simpler by omitting needless differential equations, than having a constant transcription rate for *SU(H)* mRNA, a constant rate of decay for that mRNA, constant translation of the mRNA into *SU(H)* protein, and equal decay rates for *SU(H)* protein alone or complexed with *N*. In the future, as these interactions are better elucidated, we plan to add a more detailed representation of *Su(H)* function.

Su(H) binds to the promoter region of several of the *E(spl)* complex genes, and, in the presence of activated Notch, *Su(H)* upregulates transcription of these genes [S23–S25]. In addition to *Su(H)*, these *E(spl)* genes are also activated by *Ac* and *Sc* [S8, S31, S32]. *E(spl)* proteins are bHLH transcription factors, which in turn inhibit the activity of *Ac/Da* and *Sc/Da*, both in *E(spl)* promoters and in the *ac/sc* complex promoters [S33]. Thus, *E(spl)* antagonizes its own production as well as antagonizing production of *ac/sc* complex members. The latter interaction completes the cycle from activated *N* to downregulation of the proneural genes *ac* and *sc*. For lack of evidence otherwise, we assume that *ac* and *sc* regulation is qualitatively (but not quantitatively) identical.

A few other genes appear to lie within this loop of interactions, but their function is not as well understood. There are several other bHLH activator genes such as *lethal of scute* and *atonal* that belong to the same family as *ac* and *sc* and have similar effects when overexpressed. It does not appear that these genes play as much of a role in neural selection as *ac* and *sc*, however, so we do not consider them here. Several genes related to those in the *E(spl)* complex, collectively called the *bearded* family, are activated by *ac* and *sc* [S32], and as with *E(spl)* genes, they may act as repressors of *E(spl)* and proneural activity [S34]. Lai and Posakony [S35] argue

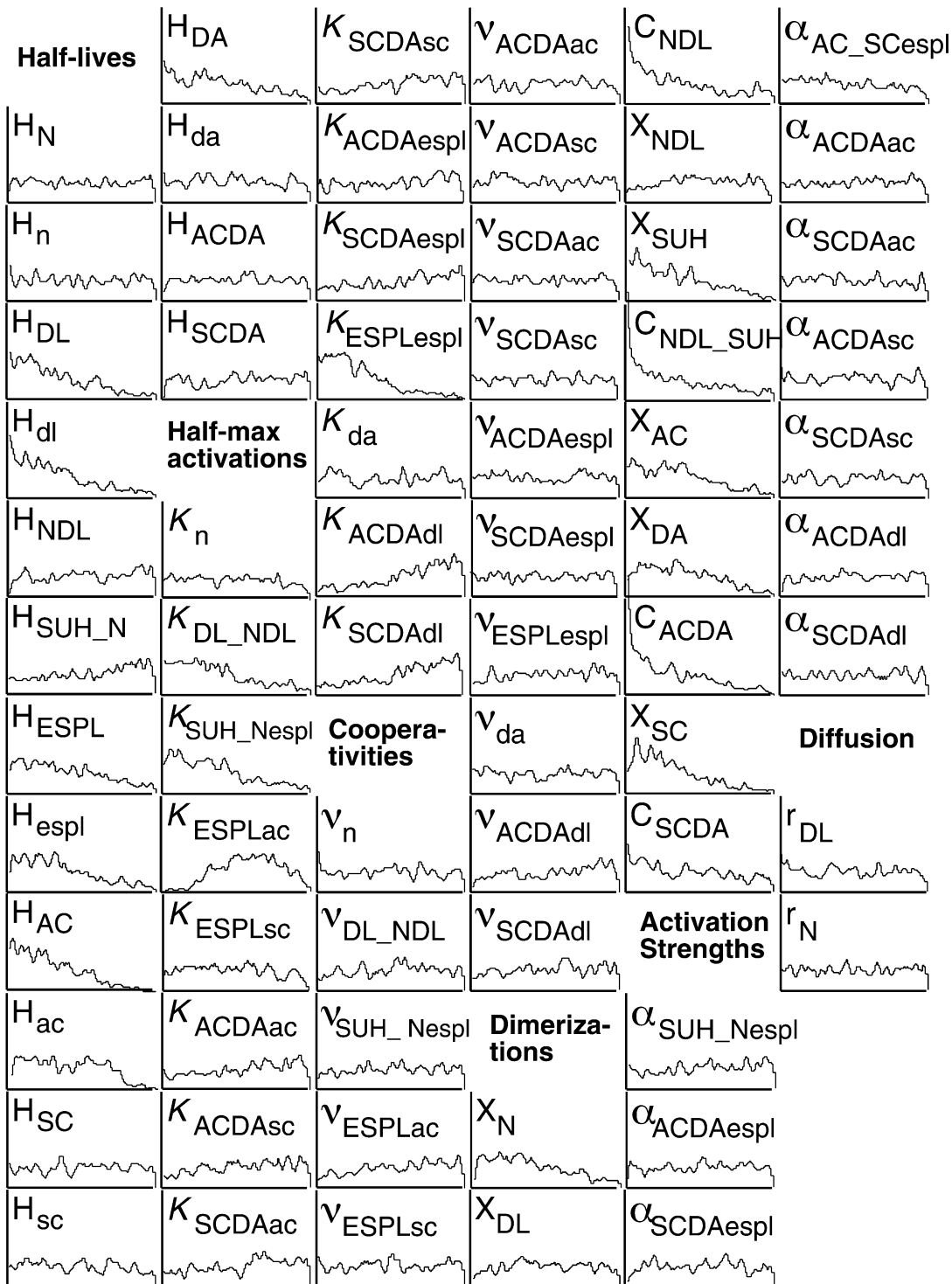


Figure S1. Histograms of Successful Parameter Values from Solutions to the Augmented Neurogenic Network with the 2-Cell Lateral Inhibition Test

Each histogram shows the values of one of the 69 parameters in the model. The horizontal axes span the range within which we picked each parameter and are plotted on a log-scale for all parameters except cooperativity (Hill) coefficients (v) and relative activator strengths (α). The vertical axes show the number of successful parameter sets in which that parameter fell within each bin along the horizontal axis. We made these plots from several hundred parameter sets. No parameter has an absolute restriction on its value, except the half-life of AC. The latter restriction arises because our test involves checking for AC concentrations close to 0 within 300 min; thus, we found no parameter sets with AC half-life > 200 min. Many other parameters, however, concentrate their values within certain ranges. We made our restricted parameter ranges based on those tendencies.

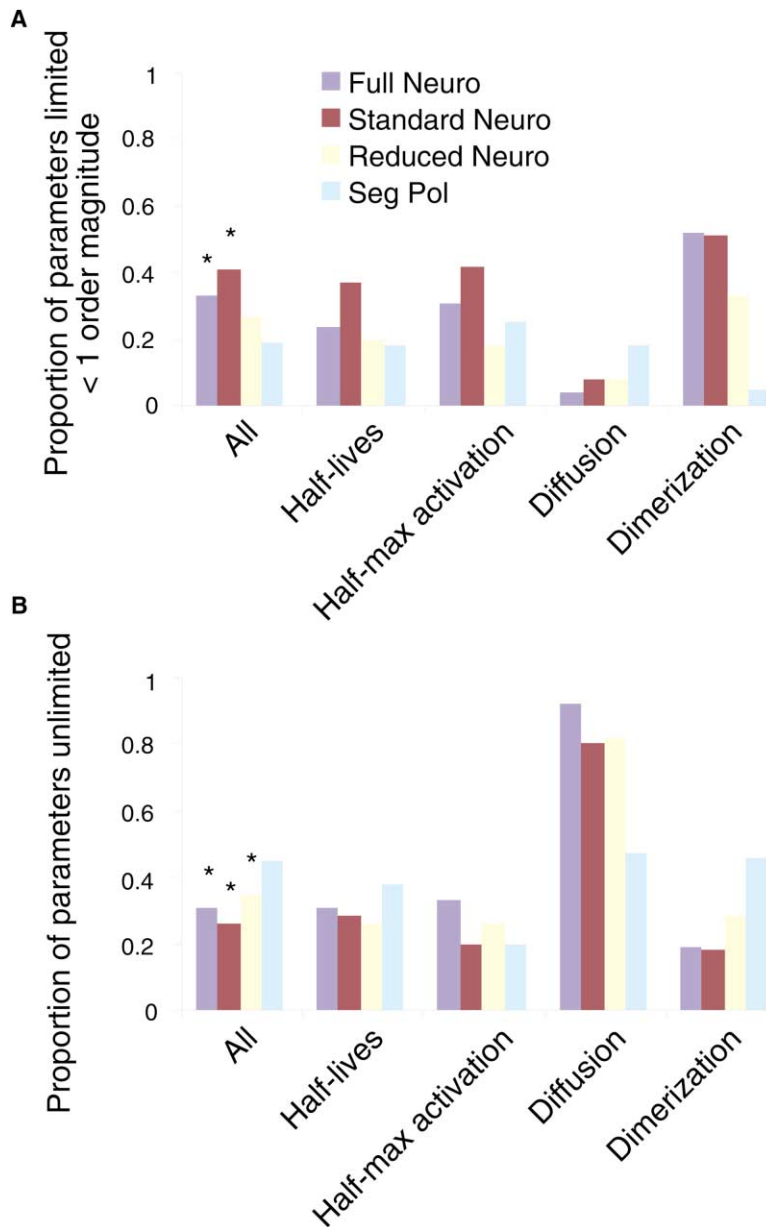


Figure S2. Sensitivity Analyses for Parameters in Each Network

We randomly selected 25 successful parameter sets that passed the 2-cell test in each of the 3 neurogenic networks and 25 successful parameter sets from the segment polarity network. For each of these, we varied each parameter individually across its full range, while holding all other parameters constant. (A) The proportion of parameters whose values could not vary by an order of magnitude around the original value without losing the ability to form the pattern.

(B) The proportion of parameters that could successfully form the pattern across the whole of their range. The colors of the bars correspond to the different networks, as indicated in the legend. In both graphs, we show results from all parameters together first, then we show results from four distinct groups of parameters. The asterisk in the “All” column indicates proportions significantly different ($p < 0.05$) from the segment polarity network. We did not perform statistics on the other columns.

that *bearded* genes repress translation rather than transcription. However, the role so far deduced for *bearded*-family genes appears to make them redundant to E(spl), so we leave them out of this first version of our model. That is, we are omitting a known redundancy, and we will therefore underestimate the robustness of the whole network.

The loop of genetic interactions outlined above is thought to be the basis of the neurogenic network’s pattern formation mechanism as follows. Initially, *ac* and *sc* are turned on in all cells of a proneural cluster by upstream genes. *Ac* and *Sc* upregulate production of *DI*. *DI* activates *N* in neighboring cells and represses *N* activity in its own cell. The activated *N* in neighboring cells, through the Su(H) and E(spl) pathway, turns off *ac* and *sc*. If one cell accumulates more *ac* or *sc* than its neighbors, either by random chance or through the action of pre patterning genes, that cell will produce more *DI* than its neighbors, causing more *N* to be activated in neighboring cells. This in turn will cause the *ac* and *sc* production in neighboring cells to decrease, increasing the difference in *ac* and *sc* concentrations in the focal cell compared to its neighbors. Once begun, this

process snowballs to high *ac* and *sc* concentrations in one focal cell and very low concentrations in all of that cell’s neighbors, thus selecting one cell out from the group.

Both *daughterless* (*da*) and *extramachrochaete* (*emc*) are bHLH proteins that form heterodimers with *Ac* and *Sc*. *Da/Ac* and *Da/Sc* heterodimers are transcriptional activators, as outlined above. *Da* homodimers are also transcriptionally active and upregulate the production of *ac* and *sc*, though in a much weaker way than *Da/Ac* and *Da/Sc* heterodimers [S7]. *Emc* lacks a DNA binding region, so it represses *Ac* and *Sc* activity by binding to them to form an inactive complex [S4, S36, S37]. *emc* [S4] does not appear to be regulated by any of the genes in the neurogenic loop. *da* is expressed ubiquitously and at fairly uniform levels throughout the tissues involved in neurogenesis [S38, S39], and we also cannot find any evidence that it is regulated by any of the genes in the neurogenic loop. *emc*, on the other hand, is expressed in a pattern complementary to that of the proneural clusters [S4]. Although neither of these is transcriptionally regulated by genes in the central loop, the concentrations of both proteins will be regulated by dimerization with *Ac* and *Sc*.

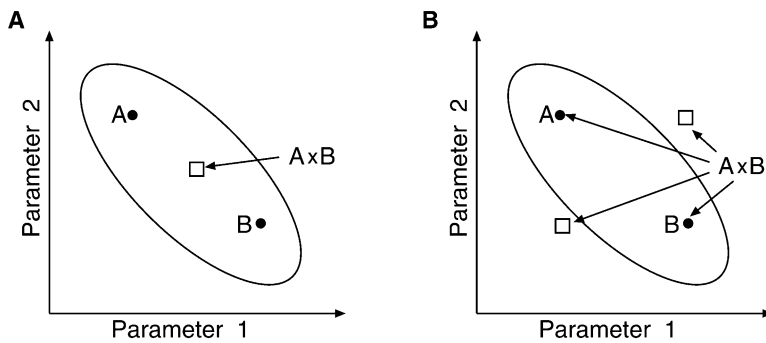


Figure S3. Two Forms of Crosses between Parameter Sets

Each parent contributes one parameter “allele” to the offspring. In sexual mating, the offspring contains both alleles, and the parameter value used by the offspring could be either one of those values (one allele is dominant) or could be an intermediate between the two.

(A) Mating parameter sets A and B, each containing two parameters, in which the offspring receives the average of its parents’ alleles.

(B) In producing gametes through meiosis, recombination between parent chromosomes produces a new chromosome that receives only one of the parent alleles, ran-

domly chosen from the two parent alleles. We chose the latter mechanism because, as shown in the diagrams, it is a stronger test of robustness; a group of parameter sets that are robust via recombination are likely also to be robust via diploid mating.

We chose to include *da*, but not *emc*, in our model, because we believed *da* should tend to make the model less stable, while *emc* should tend to make it more stable. We therefore think our study underestimates the robustness of the neurogenic network. It would be interesting to include *emc* in a future model.

Several other genes outside this central neurogenic loop appear to play important roles in the patterning of neural cells. Among these, the genes *hairy* [S40] and *Hairless* [S41] both appear to be important in laying down the prepattern for neural selection. Other less-well-studied genes, such as members of the *iroquois* complex [S42], *msh* [S43], and *vnd* [S44], are also involved in this pre-patterning or in interactions with the neurogenic genes in other patterning processes. These latter genes will not be discussed here, but the results from our study should at least partially extrapolate to them. When, in our model, we prescribe initial conditions that boost expression of Ac and Sc in one or a few cells, we assume that this bias comes from the prior action of genes like *hairy*, *Hairless*, *iroquois*, *msh*, and *vnd*.

Parameters Are Not Restricted in Their Values

Figure S1 shows histograms of the parameter values from all solutions we found while randomly searching parameter space using the 2-cell test on the augmented neurogenic network. In this search, we picked all parameters except cooperativities and activation strengths from ranges spanning at least two and often three or four orders of magnitude (the latter two spanned a single order of magnitude). For instance, the half-life of each component could range from 1 to 1000 min. Although some parameters tend to cluster in part of their range, there do not appear to be any absolute restrictions. The parameter histograms for the segment polarity network looks similar to Figure S1, with no absolute restrictions [S45]. This lack of restrictions could be due to compensation between pairs or groups of parameters. In other words, parameter A can be high as long as parameter B is low and vice versa. However, we failed to find any strong pair-wise cross-correlations for either network. We enforced some weak correlations during our parameter search to avoid physically unrealistic corners of parameter space (where the ODE integrations ran extremely slowly because of unrealistically high dimerization rates). Excluding those, the highest cross-correlations we found were on the order of $r = 0.3$. So any compensation must be relatively weak or, more likely, involve groups of more than two parameters.

The Neurogenic and Segment Polarity Networks Are Both Astonishingly Insensitive to Parameter Variation

We did traditional parameter sensitivity analyses on 25 solutions from each of our 3 neurogenic network models forming the 2-cell pattern. For comparison, we also did this sensitivity analysis on 25 solutions from the segment polarity network. In each solution, we varied one parameter at a time through 40 steps across its full range (not restricted as in the previous section) while keeping all other parameter values fixed. At each parameter value, we calculated a

quantitative score representing how close the network came to passing the test and picked a threshold for this score that separated good solutions (by our subjective judgement) from bad ones. In our previous paper on the segment polarity network, we showed that parameters could usually be varied quite far without changing the pattern [S45]. The full neurogenic network shows a slightly higher sensitivity to parameter values. We counted the number of parameters that were restricted to less than an order of magnitude variation across all solutions for each network (excluding parameters in which our original ranges were one order of magnitude or less). Whereas only 19% of parameters in the segment polarity network were limited to less than one order of magnitude variation, 33% of the full neurogenic network parameters were so restricted (Figure S2A). Conversely, 44% of the segment polarity parameters could vary across the whole range we gave for them without losing the pattern, while only 31% of the neurogenic network parameters could so vary (Figure S2B). The reduced neurogenic network showed similar sensitivities to the augmented neurogenic network. The standard neurogenic network was more sensitive to parameter variation than either of the others and was significantly more sensitive than the reduced network. These sensitivities are consistent with the success rates of randomly chosen parameter sets.

The above results indicate that the model neurogenic network may be slightly more sensitive to parameter variations than the model segment polarity network. But there are more significant differences among certain classes of parameters. The biggest difference is in parameters governing dimerizations. There are many more of these in the neurogenic network, and 50% of these parameters could not be varied by an order of magnitude around their original value (Figure S2A). By contrast, the parameters associated with the one dimerization step in the segment polarity network were only so limited 5% of the time. The segment polarity network, on the other hand, seems more sensitive to parameters governing transport processes, whereas the neurogenic network is almost completely insensitive to variations of these parameters (which in the neurogenic network only includes intracellular diffusion of D1 and N among neighboring faces of each cell). Other classes of parameters such as half-lives have similar sensitivities in both networks.

Recombination and Mutational Expansion Algorithms

Sexual mating produces offspring with one allele from each parent. The phenotype can be an equal blend of the effects of each parent allele (Figure S3A), can be determined by only the dominant allele (Figure S3B), or can lie between these extremes. In meiotic recombination, the gamete receives only one parental allele (Figure S3B). As shown in Figure S3, meiotic recombination produces offspring that are more dissimilar to the parents than a blended mating, and we thus chose this form of mating for our “recombination” test of robustness.

Mutational expansion adds an evolutionary component to the recombination test. We start with a single successful parameter set and make several offspring parameter sets by introducing $\pm 10\%$

magnitude random “mutations” in a randomly selected 10% of the parameters. These changes in value might correspond to single amino acid changes that have small effects on the binding rates of the proteins, etc. We then ask whether each of these offspring parameter sets can pass our chosen test. We keep the ones that are successful as a new group of parent parameter sets. We then recombine this generation of parents to form a new group of offspring, again introducing mutations into the parameter values of each offspring as above. After discarding the unsuccessful offspring, we keep up to 200 of the successful offspring to form the new group of parents. We aim to produce 800 successful offspring each round, from which we randomly decide which of the successful ones to keep as the next parents, with a bias favoring those whose parents who had parameter values that were most distant from each other. We introduce this bias that favors a surrogate for “hybrid vigor” to prevent our simulated population of parameter sets from contracting toward a small-diameter set (within which recombination would be successful trivially). We continue this process until less than 90% of random mating of the 200 parents results in successful offspring parameter sets. At that point, we measure the ratio between the highest and lowest value for each parameter and take the average of the ratios across all parameters as our measure of the size of the neighborhood in parameter space within which random matings almost always produce viable offspring networks. Stopping the process when fewer than 90% of matings fail (rather than 92%), or keeping the size of our population of networks hovering near 200 (rather than 400 or 10,000), etc., are details, decided by the computational capacity we have access to, that do not much matter, we believe. The following outline gives more detail on our mutational expansion algorithm.

An Outline of the Mutational Expansion Algorithm We Used to Make a Cloud of Parameter Sets that Expands around One Successful Parameter Set

1. Make eight offspring parameter sets from the original parameter set, in which each parameter in each offspring has a 10% chance of having a random multiplicative change (mutation) of up to $\pm 10\%$ in its value relative to the parent value.
2. Test each offspring parameter set for its ability to make the pattern in question, and keep only those that succeed. This creates a new pool of parent parameter sets.
3. From each new parent, create n offspring by mating that parent with another randomly chosen parent. n initially equals 8. “Mating” means randomly selecting half the parameter values from one parent and the other half from the other (Figure S3B). Also, mutate each offspring’s parameter values as in (1).
4. Test each of the new offspring for its ability to make the pattern in question, and keep only those that succeed.
5. If there are more than 200, decide randomly which to keep, but with a bias favoring those whose parents were farthest apart in parameter space. Distance is a scaled Euclidean distance between the parameter vectors of each parent, where each parameter’s value is scaled between 0 and 1 based on the ranges we used when picking that parameter’s value randomly.
6. If there were less than 800 successful offspring, increase n by 1. If there were more than 800 successful offspring, decrease n by 1.
7. Repeat 3–6 until the percentage of offspring that are successful falls below 90%.

A Proposal for How to Conduct a Saturating Search for Robust Neighborhoods in Parameter Space

The parameter space in gene network models is huge (i.e., of large dimension). No realistic depiction of gene networks can possibly escape this difficulty. With 69 parameters, it would be just barely possible to explore all combinations of a high and a low value for each parameter on one of our lab’s current computers within the lifetime of the universe. Therefore, in order to explore gene network models at all, we need either to be lucky enough to work with extraordinarily robust networks, as we have been lucky so far, or we need sophisticated methods for navigating parameter space. The following mutational expansion method we propose for finding

the robustness to parameter variation is a prototype for a technique that should be practically computable. We start with one successful parameter set and use mutational expansion to find a cloud of parameter sets around this first one. When we have expanded the cloud as far as possible, we randomly find a new successful parameter set. We then cross this new parameter set with all the parameter sets in the first cloud. If the new one crosses successfully with a large proportion of the cloud, we add it to the cloud. If it cannot cross successfully with most parameter sets in the cloud, we assume that it lies outside the cloud. In the latter case, we use mutational expansion to find a cloud of parameter sets around this new set. We now have two distinct clouds of successful parameters in the space. We continue to pick new random successful parameters, mating them with each of the existing clouds, and forming a new cloud around those that cannot successfully mate with any existing clouds. This is analogous to the Gram-Schmidt orthonormalization procedure.

If there are a small number of good regions in the parameter space, then the probability that a new random parameter set will not belong to an already existing cloud will decrease over time. By extrapolating the curve of this probability over the number of random parameter sets sampled, we can make a good guess at how many distinct successful neighborhoods are contained in the parameter space and perhaps find the majority of the largest ones.

Based on the limited number of mutational expansion computations we did, the procedure outlined above would certainly take vast computational resources, but potentially an amount that a reasonable budget could afford. The process outlined here would be easiest in the case of a network for which solutions were easily found by random search, as for our models of the segment polarity and neurogenic networks, but would be a valuable assessment no matter how one discovered the founder sets. The end result would be a description of how many qualitatively different ways a network can form a particular pattern and how far apart these different strategies are from each other. This is interesting both evolutionarily and practically. From an evolutionary perspective, these neighborhoods define the adaptive landscape within which natural selection functions. From a more practical perspective, measuring the values of parameters in a genetic network is hard and almost never done. It is unlikely that anyone will ever measure all 69 parameters in our full neurogenic network. But, to find the neighborhood in parameter space in which the real network sites might be possible after measuring only a few parameter values. The above analysis tells the experimentalist which parameters are most important to measure in order to distinguish between the different potential mechanisms.

We finish this discussion with an appeal to mathematicians for help. The abstract concept we advance above is to find (by some computation, practical in high-dimensional parameter space) boundaries of the largest possible neighborhood surrounding a single “founder” parameter set within which network function would be heritable through random recombinatorial mating, then to use some measure of the volume/shape of that neighborhood as a biologically meaningful measure of network robustness (in the vicinity of the founder parameter set). The computational algorithm for finding this neighborhood need have no biological realism. We indeed used a computational algorithm whose steps mimic evolution to feel out the neighborhood, because we suspect that we cannot do better than to emulate natural selection. It has been navigating such parameter spaces for billions of years and has likely found an efficient method to wend its way. But algorithms other than what we used might be much faster on computers.

In addition to the challenge of conceiving a good computational algorithm, there is a conceptually deeper problem whose solution eludes us so far. Above, we sketch one possible approach to the following challenge in topology/dynamical systems: to assess the robustness of a dynamical systems model of a genetic network, characterize the shapes, sizes, and arrangements of loci in parameter space within which the model not only performs some function robustly, but also works as well for almost all the possible offspring parameter sets. This characterization of a zone of robust function bears some resemblance to the standard concept of convexity. The concept of structural stability is almost relevant here, but not quite, because whether or not the “right” pattern forms does not hinge on

the signs of eigenvalue real parts at critical points of the dynamical system. This is because we accept time-oscillatory solutions (limit cycles or strange attractors) as “successful” patterns, provided the attractors have sufficiently small amplitude. What we really need is a formal way to define, from a network’s connections, a topology on the parameter vector space whose open neighborhoods delineate who can breed with whom to produce “viable” offspring (networks). Different points in the parameter space will cause the dynamical system to make different ensembles of spatial patterns (i.e., different attractors). Some points will cause the system to have no attractors at all. Thus, we suspect that, in order to define the topology we seek, we must first pick a particular pattern (attractor) and understand that different patterns induce different topologies on parameter space. In any case, what we seek are ideas for defining a proper topology on parameter space whose open neighborhoods correspond formally to our casual use of the term neighborhoods in the main text.

The Equations for the Augmented Model

The equations in the models presented here use the same general formulation and nondimensionalization as in von Dassow et al. (2000) [S45] and further described in [S46]. Using those forms, here are the equations for the augmented model discussed in the paper.

We represent transcriptional activation by a single activator using a sigmoidal function:

$$\phi(X, \kappa_X, \nu_X) = \left(\frac{X^{\nu_X}}{\kappa^{\nu_X} + X^{\nu_X}} \right), \quad (1)$$

where X represents the activator concentration, κ is the activator concentration at which transcription proceeds at half its maximal rate, and ν is the degree of nonlinearity in the activation function (which we refer to as cooperativity). The concentrations of each element in the model are scaled so that 1 is the maximum achievable concentration, and likewise the production terms are scaled so that 1 is their maximum value. We then represent repression with a backward sigmoid function:

$$\Psi(X, \kappa_X, \nu_X) = 1 - \phi(X, \kappa_X, \nu_X), \quad (2)$$

where production of an mRNA species is controlled by more than one activator; we use a probabilistic formulation to combine these activators [S46]:

$$\begin{aligned} \Gamma(X_1, X_2, X_3, \dots) &= \\ 1 - \left(1 - \frac{\alpha_1}{\text{Max}(\alpha_1, \alpha_2, \dots)} \phi(X_1, \kappa_{X_1}, \nu_{X_1}) \right) &\left(1 - \frac{\alpha_2}{\text{Max}(\alpha_1, \alpha_2, \dots)} \phi(X_2, \kappa_{X_2}, \nu_{X_2}) \right) \dots \\ &= 1 - \prod_i \left(1 - \frac{\alpha_i}{\text{Max}(\alpha)} \phi(X_i, \kappa_{X_i}, \nu_{X_i}) \right). \end{aligned} \quad (3)$$

Using these formulas, here are the full equations for the augmented model discussed in the paper. We use the above formulas as a shorthand, with the assumption that all parameters in the formulas above are included (for instance, $\Gamma(X, Y)$ would have a κ , ν , and α for each of the species X and Y). The subscript “i” indicates the cell number, and the subscript “j” indicates the face of the cell for membrane-bound components (each cell has six faces).

$$\frac{dn_i}{d\tau} = \frac{T_0}{H_n} (\phi(\text{Const}_i, \kappa_n, \nu_n) - n) \quad (4)$$

$$\frac{dN_{ij}}{d\tau} = T_0 \left[\frac{1}{H_{DL}} \left(\frac{n_i}{6} - N_{ij} \right) - C_{NDL} X_{DL} N_{ij} DL_{opp} \Psi(DL_{ij}, \kappa_{DL_NDL}, \nu_{DL_NDL}) \right] \quad (5)$$

$$\frac{dl_i}{d\tau} = \frac{T_0}{H_{dl}} (\Gamma(\text{ACDA}, \text{SCDA}) - dl_i) \quad (6)$$

$$\frac{dDL_{ij}}{d\tau} = T_0 \left[\frac{1}{H_{DL}} \left(\frac{dl_i}{6} - DL_{ij} \right) - C_{NDL} X_{DL} DL_{ij} N_{opp} \Psi(DL_{opp}, \kappa_{DL_NDL}, \nu_{DL_NDL}) \right] \quad (7)$$

$$\frac{dNDL_{ij}}{d\tau} = T_0 \left[\frac{-NDL_{ij}}{H_{NDL}} + C_{NDL} X_{DL} N_{ij} DL_{opp} \Psi(DL_{ij}, \kappa_{DL_NDL}, \nu_{DL_NDL}) \right] \quad (8)$$

$$\frac{dac_i}{d\tau} = \frac{T_0}{H_{bc}} (\Gamma(\text{ACDA}, \text{SCDA}) \Psi(\text{ESPL}_i, \kappa_{\text{ESPL}_{bc}}, \nu_{\text{ESPL}_{bc}}) - ac_i) \quad (9)$$

$$\frac{dAC_i}{d\tau} = T_0 \left[\frac{1}{H_{AC}} (ac_i - AC_i) - C_{ACDA} X_{DA} AC_i DA_i \right] \quad (10)$$

$$\frac{dsc_i}{d\tau} = \frac{T_0}{H_{sc}} (\Gamma(\text{ACDA}, \text{SCDA}) \Psi(\text{ESPL}_i, \kappa_{\text{ESPL}_{sc}}, \nu_{\text{ESPL}_{sc}}) - sc_i) \quad (11)$$

$$\frac{dSC_i}{d\tau} = T_0 \left[\frac{1}{H_{SC}} (sc_i - SC_i) - C_{SCDA} X_{DA} SC_i DA_i \right] \quad (12)$$

$$\frac{dda_i}{d\tau} = \frac{T_0}{H_{da}} (\phi(\text{Const}_i, \kappa_{da}, \nu_{da}) - da_i) \quad (13)$$

$$\frac{dDA_i}{d\tau} = T_0 \left[\frac{1}{H_{DA}} (da_i - DA_i) - C_{ACDA} X_{AC} AC_i DA_i - C_{SCDA} X_{SC} SC_i DA_i \right] \quad (14)$$

$$\frac{despl_i}{d\tau} = \frac{T_0}{H_{espl}} \left[\Gamma[\text{SUH}_N, [\Gamma(\text{ACDA}, \text{SCDA}) \Psi(\text{ESPL}_i, \kappa_{\text{ESPL}_{espl}}, \nu_{\text{ESPL}_{espl}})]] - espl_i \right] \quad (15)$$

$$\frac{dESPL_i}{d\tau} = \frac{T_0}{H_{ESPL}} (espl_i - \text{ESPL}_i) \quad (16)$$

$$\frac{dACDA_i}{d\tau} = T_0 \left[\frac{-ACDA_i}{H_{ACDA}} + C_{ACDA} X_{DA} AC_i DA_i \right] \quad (17)$$

$$\frac{dSCDA_i}{d\tau} = T_0 \left[\frac{-SCDA_i}{H_{SCDA}} + C_{SCDA} X_{DA} SC_i DA_i \right] \quad (18)$$

$$\frac{dSUH_i}{d\tau} = T_0 \left[\frac{\text{SUH}_N}{H_{\text{SUH}_N}} - C_{NDL_SUH} X_{NDL} NDL_i \text{SUH}_i \right] \quad (19)$$

$$\frac{d\text{SUH}_N}{d\tau} = T_0 \left[\frac{-\text{SUH}_N}{H_{\text{SUH}_N}} + C_{NDL_SUH} X_{\text{SUH}} NDL_i \text{SUH}_i \right] \quad (20)$$

$$\frac{d\text{Const}_i}{d\tau} = 0 \quad (21)$$

Supplementary References

- S1. Campuzano, S., and Modolell, J. (1992). Patterning of the *Drosophila* nervous system: the achaete-scute gene complex. *Trends Genet.* 8, 202–208.
- S2. Gigliani, F., Longo, F., Gaddini, L., and Battaglia, P.A. (1996). Interactions among the bHLH domains of the proteins encoded by the Enhancer of split and achaete-scute gene complexes of *Drosophila*. *Mol. Gen. Genet.* 251, 628–634.

- S3. Alifragis, P., Poortinga, G., Parkhurst, S.M., and Delidakis, C. (1997). A network of interacting transcriptional regulators involved in *Drosophila* neural fate specification revealed by the yeast two-hybrid system. *Proc. Natl. Acad. Sci. USA* **94**, 13099–13104.
- S4. Van Doren, M., Powell, P.A., Pasternak, D., Singson, A., and Posakony, J.W. (1992). Spatial regulation of proneural gene activity: auto- and cross-activation of achaete is antagonized by extramacrochaetae. *Genes Dev.* **6**, 2592–2605.
- S5. Skeath, J.B., and Carroll, S.B. (1991). Regulation of achaete-scute gene expression and sensory organ pattern formation in the *Drosophila* wing. *Genes Dev.* **5**, 984–995.
- S6. Martinez, C., and Modolell, J. (1991). Cross-regulatory interactions between the proneural achaete and scute genes of *Drosophila*. *Science* **251**, 1485–1487.
- S7. Cabrera, C.V., and Alonso, M.C. (1991). Transcriptional activation by heterodimers of the achaete-scute and daughterless gene products of *Drosophila*. *EMBO J.* **10**, 2965–2973.
- S8. Hinz, U., Giebel, B., and Campos-Ortega, J.A. (1994). The basic-helix-loop-helix domain of *Drosophila* lethal of scute protein is sufficient for proneural function and activates neurogenic genes. *Cell* **76**, 77–87.
- S9. Kunisch, M., Haenlin, M., and Campos-Ortega, J.A. (1994). Lateral inhibition mediated by the *Drosophila* neurogenic gene delta is enhanced by proneural proteins. *Proc. Natl. Acad. Sci. USA* **91**, 10139–10143.
- S10. Haenlin, M., Kunisch, M., Kramatschek, B., and Campos-Ortega, J.A. (1994). Genomic regions regulating early embryonic expression of the *Drosophila* neurogenic gene Delta. *Mech. Dev.* **47**, 99–110.
- S11. Fehon, R.G., Kooh, P.J., Rebay, I., Regan, C.L., Xu, T., Muskavitch, M.A., and Artavanis-Tsakonas, S. (1990). Molecular interactions between the protein products of the neurogenic loci Notch and Delta, two EGF-homologous genes in *Drosophila*. *Cell* **61**, 523–534.
- S12. Heitzler, P., and Simpson, P. (1993). Altered epidermal growth factor-like sequences provide evidence for a role of Notch as a receptor in cell fate decisions. *Development* **117**, 1113–1123.
- S13. de Celis, J.F., and Bray, S. (1997). Feed-back mechanisms affecting Notch activation at the dorsoventral boundary in the *Drosophila* wing. *Development* **124**, 3241–3251.
- S14. Klein, T., Brennan, K., and Arias, A.M. (1997). An intrinsic dominant negative activity of serrate that is modulated during wing development in *Drosophila*. *Dev. Biol.* **189**, 123–134.
- S15. Klueg, K.M., Parody, T.R., and Muskavitch, M.A. (1998). Complex proteolytic processing acts on Delta, a transmembrane ligand for Notch, during *Drosophila* development. *Mol. Biol. Cell* **9**, 1709–1723.
- S16. Qi, H., Rand, M.D., Wu, X., Sestan, N., Wang, W., Rakic, P., Xu, T., and Artavanis-Tsakonas, S. (1999). Processing of the notch ligand delta by the metalloprotease Kuzbanian. *Science* **283**, 91–94.
- S17. Fehon, R.G., Johansen, K., Rebay, I., and Artavanis-Tsakonas, S. (1991). Complex cellular and subcellular regulation of notch expression during embryonic and imaginal development of *Drosophila*: implications for notch function. *J. Cell Biol.* **113**, 657–669.
- S18. Seugnet, L., Simpson, P., and Haenlin, M. (1997). Transcriptional regulation of Notch and Delta: requirement for neuroblast segregation in *Drosophila*. *Development* **124**, 2015–2025.
- S19. Huppert, S.S., Jacobsen, T.L., and Muskavitch, M.A. (1997). Feedback regulation is central to Delta-Notch signalling required for *Drosophila* wing vein morphogenesis. *Development* **124**, 3283–3291.
- S20. Struhl, G., and Adachi, A. (1998). Nuclear access and action of notch in vivo. *Cell* **93**, 649–660.
- S21. Fortini, M.E., and Artavanis-Tsakonas, S. (1994). The suppressor of hairless protein participates in notch receptor signaling. *Cell* **79**, 273–282.
- S22. Hsieh, J.J., Henkel, T., Salmon, P., Robey, E., Peterson, M.G., and Hayward, S.D. (1996). Truncated mammalian Notch1 activates CBF1/RBPJk-repressed genes by a mechanism resembling that of Epstein-Barr virus EBNA2. *Mol. Cell. Biol.* **16**, 952–959.
- S23. Bailey, A.M., and Posakony, J.W. (1995). Suppressor of hairless directly activates transcription of enhancer of split complex genes in response to Notch receptor activity. *Genes Dev.* **9**, 2609–2622.
- S24. Lecourtois, M., and Schweisguth, F. (1995). The neurogenic suppressor of hairless DNA-binding protein mediates the transcriptional activation of the enhancer of split complex genes triggered by Notch signaling. *Genes Dev.* **9**, 2598–2608.
- S25. Eastman, D.S., Slee, R., Skoufos, E., Bangalore, L., Bray, S., and Delidakis, C. (1997). Synergy between suppressor of Hairless and Notch in regulation of Enhancer of split m gamma and m delta expression. *Mol. Cell. Biol.* **17**, 5620–5628.
- S26. Jimenez, G., and Ish-Horowicz, D. (1997). A chimeric enhancer-of-split transcriptional activator drives neural development and achaete-scute expression. *Mol. Cell. Biol.* **17**, 4355–4362.
- S27. Gho, M., Lecourtois, M., Geraud, G., Posakony, J.W., and Schweisguth, F. (1996). Subcellular localization of Suppressor of Hairless in *Drosophila* sense organ cells during Notch signalling. *Development* **122**, 1673–1682.
- S28. Li, Y., and Baker, N.E. (2001). Proneural enhancement by Notch overcomes Suppressor-of-Hairless repressor function in the developing *Drosophila* eye. *Curr. Biol.* **11**, 330–338.
- S29. Furriols, M., and Bray, S. (2001). A model Notch response element detects Suppressor of Hairless-dependent molecular switch. *Curr. Biol.* **11**, 60–64.
- S30. Brou, C., Logeat, F., Lecourtois, M., Vandekerckhove, J., Kourilsky, P., Schweisguth, F., and Israel, A. (1994). Inhibition of the DNA-binding activity of *Drosophila* suppressor of hairless and of its human homolog, KBF2/RBP-J kappa, by direct protein-protein interaction with *Drosophila* hairless. *Genes Dev.* **8**, 2491–2503.
- S31. Kramatschek, B., and Campos-Ortega, J.A. (1994). Neuroectodermal transcription of the *Drosophila* neurogenic genes E(spl) and HLH-m5 is regulated by proneural genes. *Development* **120**, 815–826.
- S32. Singson, A., Leviten, M.W., Bang, A.G., Hua, X.H., and Posakony, J.W. (1994). Direct downstream targets of proneural activators in the imaginal disc include genes involved in lateral inhibitory signaling. *Genes Dev.* **8**, 2058–2071.
- S33. Oellers, N., Dehio, M., and Knust, E. (1994). bHLH proteins encoded by the Enhancer of split complex of *Drosophila* negatively interfere with transcriptional activation mediated by proneural genes. *Mol. Gen. Genet.* **244**, 465–473.
- S34. Lai, E.C., Bodner, R., Kavalier, J., Freschi, G., and Posakony, J.W. (2000). Antagonism of notch signaling activity by members of a novel protein family encoded by the bearded and enhancer of split gene complexes. *Development* **127**, 291–306.
- S35. Lai, E.C., and Posakony, J.W. (1997). The Bearded box, a novel 3' UTR sequence motif, mediates negative post-transcriptional regulation of Bearded and Enhancer of split Complex gene expression. *Development* **124**, 4847–4856.
- S36. Martinez, C., Modolell, J., and Garrell, J. (1993). Regulation of the proneural gene achaete by helix-loop-helix proteins. *Mol. Cell. Biol.* **13**, 3514–3521.
- S37. Van Doren, M., Ellis, H.M., and Posakony, J.W. (1991). The *Drosophila* extramacrochaetae protein antagonizes sequence-specific DNA binding by daughterless/achaete-scute protein complexes. *Development* **113**, 245–255.
- S38. Cronmiller, C., and Cummings, C.A. (1993). The daughterless gene product in *Drosophila* is a nuclear protein that is broadly expressed throughout the organism during development. *Mech. Dev.* **42**, 159–169.
- S39. Vaessin, H., Brand, M., Jan, L.Y., and Jan, Y.N. (1994). daughterless is essential for neuronal precursor differentiation but not for initiation of neuronal precursor formation in *Drosophila* embryo. *Development* **120**, 935–945.
- S40. Van Doren, M., Bailey, A.M., Esnayra, J., Ede, K., and Posakony, J.W. (1994). Negative regulation of proneural gene activity: hairy is a direct transcriptional repressor of achaete. *Genes Dev.* **8**, 2729–2742.
- S41. Bang, A.G., Bailey, A.M., and Posakony, J.W. (1995). Hairless promotes stable commitment to the sensory organ precursor cell fate by negatively regulating the activity of the Notch signaling pathway. *Dev. Biol.* **172**, 479–494.

- S42. Leyns, L., Gomez-Skarmeta, J.L., and Dambly-Chaudiere, C. (1996). *iroquois*: a prepattern gene that controls the formation of bristles on the thorax of *Drosophila*. *Mech. Dev.* *59*, 63–72.
- S43. D'Alessio, M., and Frasch, M. (1996). *msh* may play a conserved role in dorsoventral patterning of the neuroectoderm and mesoderm. *Mech. Dev.* *58*, 217–231.
- S44. Skeath, J.B., Panganiban, G.F., and Carroll, S.B. (1994). The ventral nervous system defective gene controls proneural gene expression at two distinct steps during neuroblast formation in *Drosophila*. *Development* *120*, 1517–1524.
- S45. von Dassow, G., Meir, E., Munro, E.M., and Odell, G.M. (2000). The segment polarity network is a robust developmental module. *Nature* *406*, 188–192.
- S46. Meir, E., von Dassow, G., Munro, E., and Odell, G.M. (2002). Ingeneue: a versatile tool for reconstituting genetic networks in silico. *J. Exp. Zool.*, in press.